Supporting information for:

Development of a novel scorpionate ligand with 6-methylpyridine and comparison of structural and electronic properties of nickel(II) complexes with related tris(azolyl)borates.

Yusuke Fujiwara, Tomoaki Takayama, Jun Nakazawa, Masaya Okamura, Shiro Hikichi*

Department of Material and Life Chemistry

Faculty of Engineering

Kanagawa University

3-27-1 Rokkakubashi, Kanagawa-ku, Yokohama 221-8686, Japan

Fax: +81-45-413-9770

*E-mail: hikichi@kanagawa-u.ac.jp

EXPERIMENTAL DETAIL

1. General

Elemental analysis was performed on an Elementar Vario MICRO Cube. IR spectra were recorded on a JASCO FT/IR 4200 spectrometer for solid samples (as KBr pellet). NMR spectra were recorded on a JEOL ECA-600 spectrometer. ESI-MS spectra were recorded on a JMS-T100LC spectrometer. Cyclic voltammetry was performed on an ALS Model 600C electrochemical analyzer. GC analysis was performed on a Shimadzu GC2010 gas chromatograph with an Rtx-5 column (Restek, length=30 m, i.d.=0.25 mm, thickness=0.25 μm). UV-vis spectra were measured on a V650 spectrometer. All commercial reagents and solvents were used without further purification unless otherwise noted. Preparations of moisture and/or oxygen-sensitive compounds were performed by Schlenk technique under Ar atmosphere. Hydrogen phenyltris(4,4-dimethyl-2-oxazolynyl)borate (H-To^{M})[1] and [Ni^{II}Br(Tp*)] (**6**)[2] were prepared according to the literature.

2. Synthesis of the compounds

2.1. H[PhB(Py^{Me})$_3$] (H-**1**)

This compound was prepared by the procedure for the synthesis of H[PhB(Py^{H})$_3$] (HTpy^{H}) with some modification.[1] To a tetrahydrofuran solution of 1.3 M *i*-PrMgCl−LiCl (11.50 mL, 14.95 mmol), 2-Bromo-6-methylpyridine (1.50 mL, 13.2 mmol) was slowly added dropwise and stirred at ambient temperature for 12 h under argon. The volatiles were then removed under reduced pressure to obtain dark red solids involving 6-

methyl-2-pyridylmagnesium chloride. Under Ar atmosphere, the dark red solids were dispersed in 30 mL of CH_2Cl_2. To this suspension, $PhBCl_2$ (0.56 mL, 13.2 mmol) was added dropwise and the resulting dark red mixture was kept stirring overnight. Aqueous saturated Na_2CO_3 solution (30 mL) was added to the reaction mixture and stirring for 2 hours. Extraction with CH_2Cl_2 (60 mL × 2) gave a reddish brown organic phase that was dried over Na_2SO_4. After removal of Na_2SO_4 by filtration, the volatiles were removed under vacuum to give a dark red oil that was redissolved in diethyl ether, filtered, and evaporated to dryness. The product was further purified by flash chromatography on propylamine-modified silica gel with a gradient mixture of hexanes and acetone as the eluent. The product was obtaied as a pale red solid by evaporation, washed with H_2O, and then re-crystallization from toluene at −36°C (306 mg, 0.837 mmol, 19 % yield). Further re-crystallization from the CH_2Cl_2/*n*-hexane solution at room temperature gives a colorless plate crystal of H-**1** suitable for X-ray crystallography. ^{1}H NMR (600 MHz, CD_3CN, r.t.) δ 2.58 (s, 9H, Py-*Me*), 6.96-7.07 (m, 8H, Py-*3H*, B-*Ph*), 7.09 (d, 3H, Py-*5H*), 7.50 (t, 3H, Py-*4H*). ^{13}C NMR (150 MHz, CD_3CN, r.t.) δ 22.9 (s, Py-*Me*), 120.1 (s, Py-*3C*), 124.9 (s, *m*-*Ph*), 127,7 (s, *o*-*Ph*), 129.1 (s, Py-*5C*), 135.5 (s, Py-*4C*), 137.0 (s, Py-*2C*), 153.5 (s, *p*-*Ph*), 158.3 (m, Py-*6C*), 184.4 (m, B-*Ph*). ^{11}B NMR (128 MHz, CD_3CN, r.t.) δ −12.14. FT/IR (KBr, cm^{-1}) ν = 3058, 3014, 3017, 3004, 2991, 2951, 2919, 1616, 1585, 1573, 1562, 1517, 1484, 1440, 1428, 1402, 1369, 1246, 1176, 1148, 1090, 1032, 1010, 937, 827, 776, 763, 731, 704, 669, 634. UV-vis (CH_2Cl_2, r.t.) λ = 272 nm (ε = 17576 M^{-1} cm^{-1}). ESI-MS^+ (MeOH): *m/z* = 366 ($[H_2[PhB(Py^{Me})_3]]^+$ (H-**1** + H)). ESI-MS^- (MeOH): *m/z* = 364 ($[PhB(Py^{Me})_3]^-$ (**1**)). Elemental analysis calcd (%) for $H[PhB(Py^{Me})_3]\cdot 0.5$toluene ($C_{27.5}H_{28}BN_3$): Calc. C 80.30, H 6.86, N 10.22; found: C 80.12, H 7.04, N 10.19.

2.2. H[PhB(OC_4H_8-Py^{Me})(Py^{Me})$_2$] (H-**2**)

Under argon atmosphere, 2-Bromo-6-methylpyridine (3.20 mL, 28.1 mmol) and 100 mL of dehydrated THF were placed in a 200 mL two-necked flask and cooled to –80°C. To this was added 1.56 M n-BuLi/hexane solution (18.12 mL, 28.27 mmol) slowly dropwise. After stirring for 25 min, $PhBCl_2$ (1.22 mL, 9.40 mmol) was added slowly dropwise and stirred for another 10 min. The solution was stirred and allowed to warm from –80°C to ambient temperature overnight, after which the solvent was removed under reduced pressure. The residue was then dissolved in CH_2Cl_2 and desalted by filtration through Celite pad. The resulting solution was transferred to a separating funnel and washed with pure water. The organic layer was collected, dehydrated with Na_2SO_4, filtered through Celite, and the solvent was removed. Drying under reduced pressure afforded a black-brown oily substance (3.803 g, 8.69 mmol, 92 % yield). ^{1}H HNR (500 MHz, CD_3CN, r.t.) δ 1.63 (q, 2H, $OCH_2CH_2CH_2CH_2$), 1.82 (q, 2H, $OCH_2CH_2CH_2CH_2$), 2.43 (s, 3H, OBuPy-*Me*), 2.72 (d, 2H, $OCH_2CH_2CH_2CH_2$), 3.20 (d, 2H, $OCH_2CH_2CH_2CH_2$), 6.86 (d, 1H, OBuPy-*3H*), 7.00 (m, 4H, OBuPy-*5H*, *m*-*Ph*, *p*-*Ph*), 7.10 (d, 2H, Py-*3H*), 7.25 (d, 2H, Py-*5H*), 7.52 (m, 3H, OBuPy-*4H*, *o*-*Ph*), 7.67 (t, 2H, Py-*4H*). ESI-MS^- (MeOH): *m/z* = 436 ($[PhB(OC_4H_8Py^{Me})(Py^{Me})_2]^-$ (**2**)).

2.3. [Co[PhB(OEt)(Py^{Me})(Py^{Me}H)]Cl_2] (**3**)

A THF solution (30 mL) of H-**2** (744 mg) was added to a THF solution of $CoCl_2\cdot 6H_2O$ (260 mg, 2.10 mmol) and the resulting reaction mixture was stirred for 4 h under Ar at room temperature. The volatiles

were evaporated, and the residue was re-dissolved in CH_2Cl_2. The solution was then passed through a filter with Celite pad to remove insoluble components. After evaporation of CH_2Cl_2, the obtained green-blue solid was dissolved in EtOH and cooled at −36°C. After the removal of the insoluble components by filtration, the volatiles were removed by evaporation. The resulting compound was extracted with Et_2O and then the volatiles were removed under reduced pressure. The obtained blue solids were dissolved in EtOH. Refrigeration of the concentrated EtOH solution at −36°C afforded crude cobalt complexes as a blue powder (92.4 mg). Blue plate single crystals of **3** suitable for X-ray analysis were obtained by the vapor diffusion method, i.e. Et_2O vapor was diffused into a *n*-hexane solution of **3** at room temperature. ESI-MS$^+$ (MeOH) *m/z* = 305 ([PhB(Py^{Me})$_2$ + MeOH + H]$^+$ (H-**2** – $OC_4H_8Py^{Me}$ + MeOH)), 319 ([PhB(Py^{Me})$_2$ + EtOH + H]$^+$ (H-**2** – $OC_4H_8Py^{Me}$ + EtOH)), 412 ([Co^{II}[PhB(OEt)(Py^{Me})(Py^{Me}H)]Cl]$^+$ (**3** – Cl)).

2.4. [$Ni^{II}Br(Tpy^{Me})$] (4)

A solution of $HTpy^{Me}$ (0.3892 g, 1.065 mmol) in THF (10 mL) was added slowly to sodium hydride (48.9 mg, 1.223 mmol) suspended in THF (10 mL) through a cannula at 0°C. The reaction mixture was stirred for 2 h after the generation of hydrogen gas had ceased. The resulting $NaTpy^{Me}$ solution was added slowly to $NiBr_2$(glyme) (371 mg, 1.20 mmol; glyme denotes 1,2-dimethoxyethane) suspended in THF (30 mL), and the resultant mixture was stirred for 12 h at ambient temperature. After removal of the solvent under reduced pressure, the resulting solid was dissolved in CH_2Cl_2 and insoluble materials were removed by filtration through a Celite plug. The solvent was evaporated under reduced pressure and the resulting solid was washed with MeCN, *n*-hexane and then pure H_2O to obtain the purple solid of **4** (138 mg, 0.274 mmol, 26 % yield). Purple plate-shaped single crystals of **4** suitable for X-ray analysis were obtained by the vapor diffusion method, i.e. Et_2O vapor was diffused into a *n*-hexane solution of **4** at room temperature. FT/IR (KBr, cm^{-1}): ν = 3065, 3055, 3011, 2996, 2927, 1714, 1590, 1561, 1445, 1376, 1255, 1211, 1190, 1165, 1153, 1107, 1036, 1018, 1003, 921, 807, 782, 771, 732, 713, 685, 669, 650, 630, 609, 566, 535, 512, 475, 437, 421. UV-vis (CH_2Cl_2) λ = 484 nm (ε = 260 M^{-1} cm^{-1}), 586 nm (ε = 51 M^{-1} cm^{-1}), 840 nm (ε = 127 M^{-1} cm^{-1}). UV-vis (MeCN) λ = 483 nm (ε = 221 M^{-1} cm^{-1}), 581 nm (ε = 48 M^{-1} cm^{-1}), 839 nm (ε = 105 M^{-1} cm^{-1}). ESI-MS$^+$ (MeOH) *m/z* = 422 ([$Ni^{II}(Tpy^{Me})$]$^+$ (**4** – Br)), 454 ([$Ni^{II}(Tpy^{Me})$(MeOH)]$^+$ (**4** – Br + MeOH)). Elemental analysis calcd (%) for [$Ni^{II}Br(Tpy^{Me})$] ($C_{24}H_{23}BBrN_3Ni$): Calc. C 57.32, H 4.61, N 8.36; found: C 57.41, H 4.72, N 8.38.

2.5. [$Ni^{II}Br(To^{M})$] (5)

A solution of HTo^{M} (1.472 g, 3.84 mmol) in tetrahydrofuran (THF, 40 mL) was added slowly to sodium hydride (0.153 g, 3.82 mmol) suspended in THF (40 ml) through a cannula at 273 K. The reaction mixture was stirred for 2 h after the generation of hydrogen gas had ceased. The solvent was removed under reduced pressure. The resulting solid was suspended in pentane, with stirring for 10 min, and then the liquid was decanted. This was repeated twice to yield a pale-yellow powder of $NaTo^{M}$. $NaTo^{M}$ is hygroscopic (i.e. hydrolyzed to HTo^{M}) and so the solid obtained was used in the following reactions without further purification. A solution of $NaTo^{M}$ (584 mg, 1.44 mmol) in THF (30 ml) was added slowly to $NiBr_2$(glyme) (451 mg, 1.46 mmol) suspended in THF (50 mL), and the resultant mixture was stirred for 1 h at ambient temperature. After

removal of the solvent under reduced pressure, the resulting solid was dissolved in CH_2Cl_2 and insoluble materials were removed by filtration through a Celite plug. The solvent was evaporated under reduced pressure and the resulting solid was dissolved in MeCN. Refrigeration of this MeCN solution at −30°C afforded a pink powder of **5** (656 mg, 1.26 mmol, 90% yield). Pale red–pink single crystals of **5** suitable for X-ray analysis were obtained by the vapor diffusion method, i.e. *n*-hexane vapor was diffused into a $CHCl_3$ solution of **5** at room temperature. FT/IR (KBr, cm^{-1}): ν = 3075, 3049, 2967, 2901, 2872, 1598, 1462, 1435, 1388, 1369, 1353, 1277, 1194, 1166, 990, 957, 894, 846, 815, 750, 711, 671, 658, 640, 620. UV-vis (CH_2Cl_2) λ = 494 nm (ε = 349 M^{-1} cm^{-1}), 829 nm (ε = 104 M^{-1} cm^{-1}). ESI-MS^+ (MeOH) *m/z* = 522 ([$Ni^{II}Br(To^M)$] + H^+ (**5** + H)). Elemental analysis calcd (%) for [$Ni^{II}Br(To^M)$] ($C_{21}H_{29}BBrN_3NiO_3$): Calc. C 48.42, H 5.61, N 8.07; found: C 47.74, H 5.78, N 7.70.

2.6. [$Ni^{II}Cl(Tpy^{Me})$] (7)

Complex **7**, the nickel-chlorido complex with Tpy^{Me}, was synthesized using same procedure for the bromide complex **4**. Pink solids of **7** (60.4 g, 0.133 mmol, 8.9 % yield) were synthesized by reacting $NiCl_2$(glyme) (374 mg; 1.70 mmol) with in situ generated $NaTpy^{Me}$ obtained by treatment of $HTpy^{Me}$ (540 mg, 1.48 mmol) with NaH (70.1 mg; 1.75 mmol). Purple plate-shaped single crystals of **7** suitable for X-ray analysis were obtained by slow diffusion of *n*-hexane to the CH_2Cl_2 solution of **7** at room temperature. FT/IR (KBr, cm^{-1}): ν = 3083, 3064, 3043, 3010, 2996, 2974, 2927, 1591, 1562, 1445, 1377, 1255, 1210, 1189, 1163, 1151, 1106, 1067, 1033, 1020, 997, 963, 934, 922, 866, 835, 808, 784, 770, 733, 714, 686, 650, 630, 599, 566, 540, 507, 486, 455. UV-vis (CH_2Cl_2) λ = 473 nm (ε = 228 M^{-1} cm^{-1}), 548 nm (ε = 86 M^{-1} cm^{-1}), 830 nm (ε = 119 M^{-1} cm^{-1}). UV-vis (MeCN) λ = 472 nm (ε = 180 M^{-1} cm^{-1}), 560 nm (ε = 48 M^{-1} cm^{-1}), 853 nm (ε = 73 M^{-1} cm^{-1}). ESI-MS^+ (MeOH) *m/z* = 422 ([$Ni^{II}(Tpy^{Me})$]$^+$ (**7** – Cl)), 454 ([$Ni^{II}(Tpy^{Me})$(MeOH)]$^+$ (**7** – Cl + MeOH)). Elemental analysis calcd (%) for [$Ni^{II}Cl(Tpy^{Me})$]·H_2O ($C_{24}H_{25}BN_3ClNiO$): Calc. C 60.50, H 5.29, N 9.17; found: C 60.07, H 4.93, N 8.59.

3. X-ray Crystallography

The diffraction data of a crystal **1**, **3**, **4**, and **7** were collected on a Rigaku XtaLAB Synergy-R/DW system, HyPix diffractometer equipped with confocal monochromated Cu-Kα radiation, and the data were processed using CrysAlisPro (Rigaku) with Olex2[3] software. The diffraction data of **3** were collected on a Rigaku Saturn 70 CCD area detector system with graphite monochromated Mo-Kα radiation. Data collection and processing were performed using Rigaku CrystalClear software.[4]

The structures of **1**, **3**, **4,** and **7** were solved with the SHELXT[5] structure solution program using Intrinsic Phasing and refined with the SHELXL-2018/3[6] refinement package using Least Squares minimization. The structure of **5** was solved by a direct method on SIR-92[7] and refinement by full-matrix least squares (SHELXL-2014/7)[8] were performed on WinGX[9] software. All non-hydrogen atoms were refined anisotropically and refined with a riding model with U_{iso} constrained to be 1.2 times U_{eq} of the carrier atom. Crystal Information Files (CIF) of the complexes reported in this paper have been deposited with the Cambridge Crystallographic

Data Centre as supplementary publications CCDC 2172875-2172879. These data can be obtained free of charge from The Cambridge Crystallographic Data Centre at www.ccdc.cam.ac.uk/data_request/cif.

4. DFT calculations

Calculations were performed using the DFT method implemented in the Gaussian 16 package of programs[10]. The structures were fully optimized using the UB3LYP method. All calculations were performed using the scalar relativistic contracted versions of the def2-TZVP (Ni) and def2-SVP (C, H, B, N, and Br) basis sets[11]. The structural optimization was performed by reading the coordinate data from the crystal structure, and the resulting molecular orbitals were visualized using Gauss View 6 programs[12]. All calculations employ Tight SCF convergence criteria and were performed using the polarizable continuum model (PCM)[13] to compute the structures in solutions. The excited states were calculated using the TD-DFT[14] method within the Tamm-Dancoff approximation as implemented in Gaussian 16. These calculations employ the hybrid UB3LYP functional along with the basis sets described above. At least 100 excited states were computed in each calculation.

5. Procedure of the catalytic reactions

A solution of the nickel compounds (2.0 μmol), cyclohexane (15.0 mmol) in MeCN (1 mL), and CH_2Cl_2 (1 mL) was placed in a Schlenk tube and degassed with Ar gas. Next, a CH_2Cl_2 (2 mL) solution of *m*CPBA (2.0 mmol) was added under Ar atmosphere and stirred at an appropriate temperature (25°C). To monitor product formation, 0.2 mL of the reaction mixture was corrected at certain times (reaction time 0, 10, 30, 60, 120, 180 min) and quenched with a dichloromethane solution (0.5 mL) of triphenylphosphine (10 mg), and then the solution was subjected to GC analysis.

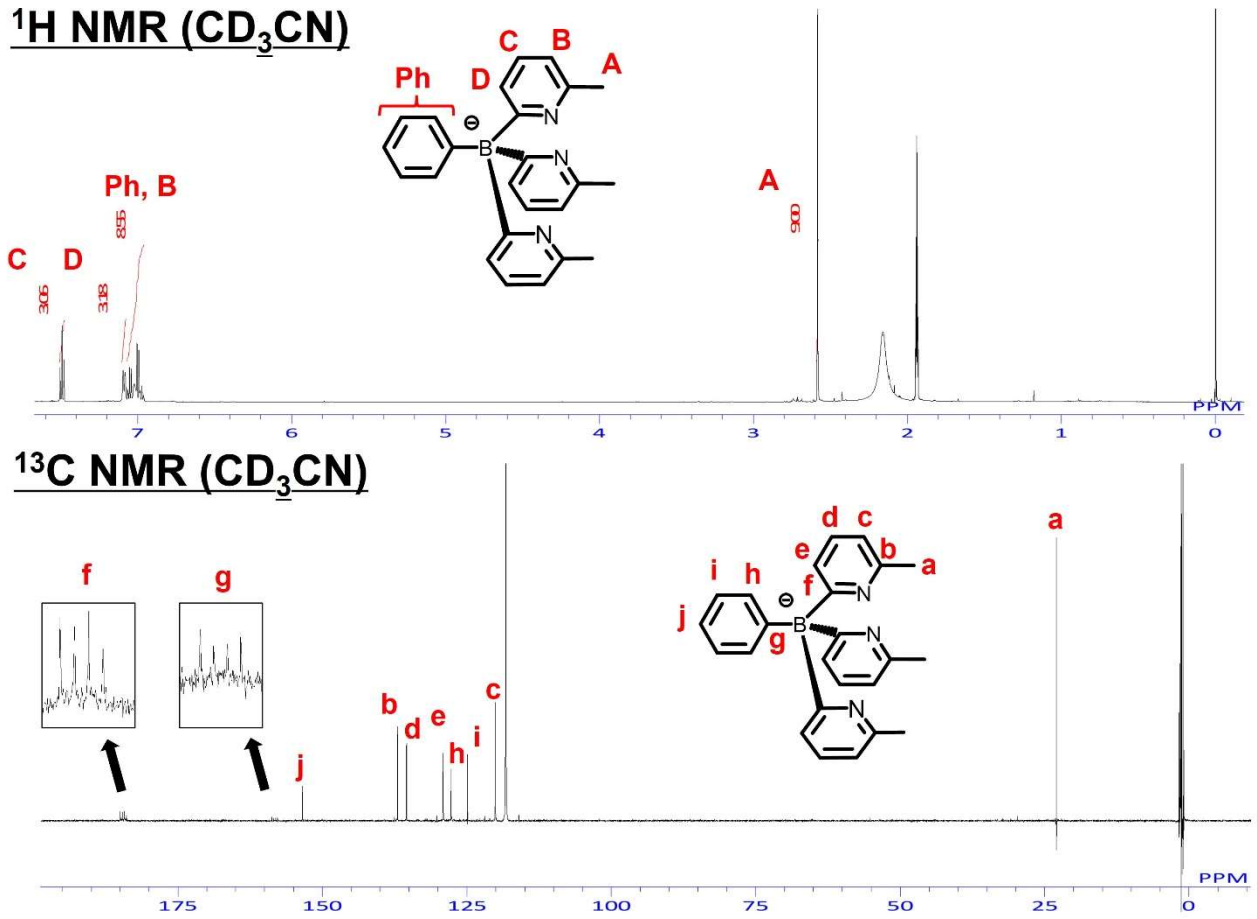

Fig. S1 ^{1}H (top; 600 MHz) and ^{13}C (bottom; 150 MHz) NMR spectra of H[PhB(Py^{Me})$_3$] (H-**1**) in CD_3CN at room temperature.

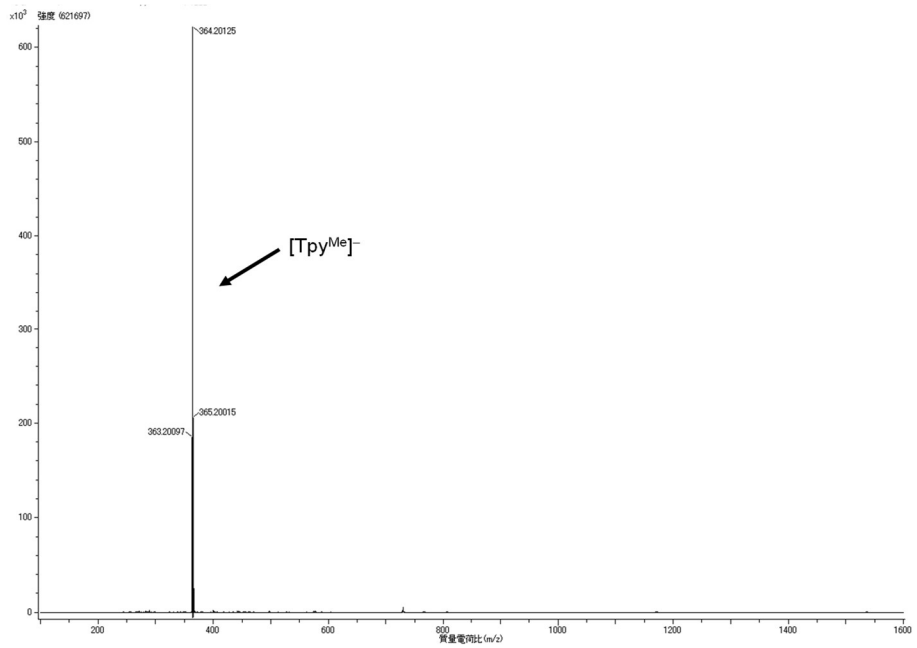

Fig. S2 ESI-MS(–) spectrum of H[PhB(Py^{Me})$_3$] (H-**1**) in MeOH.

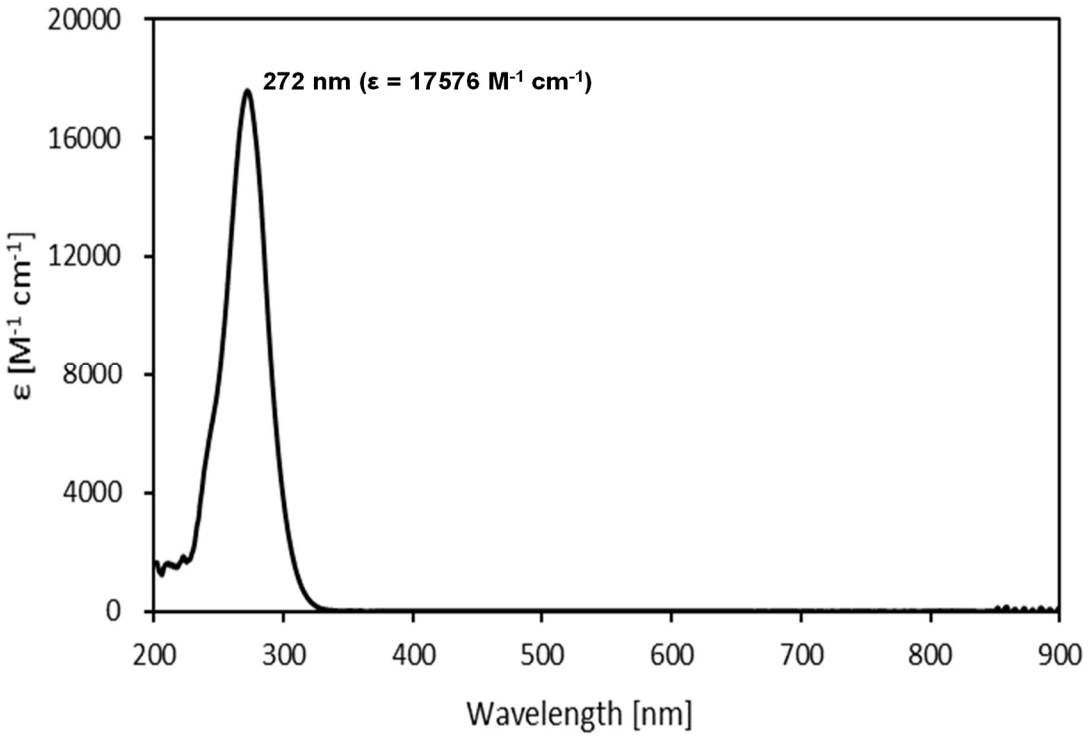

Fig. S3 UV-vis spectrum of H[PhB(Py^{Me})$_3$] (H-**1**) in CH_2Cl_2 (0.052 mM) at room temperature.

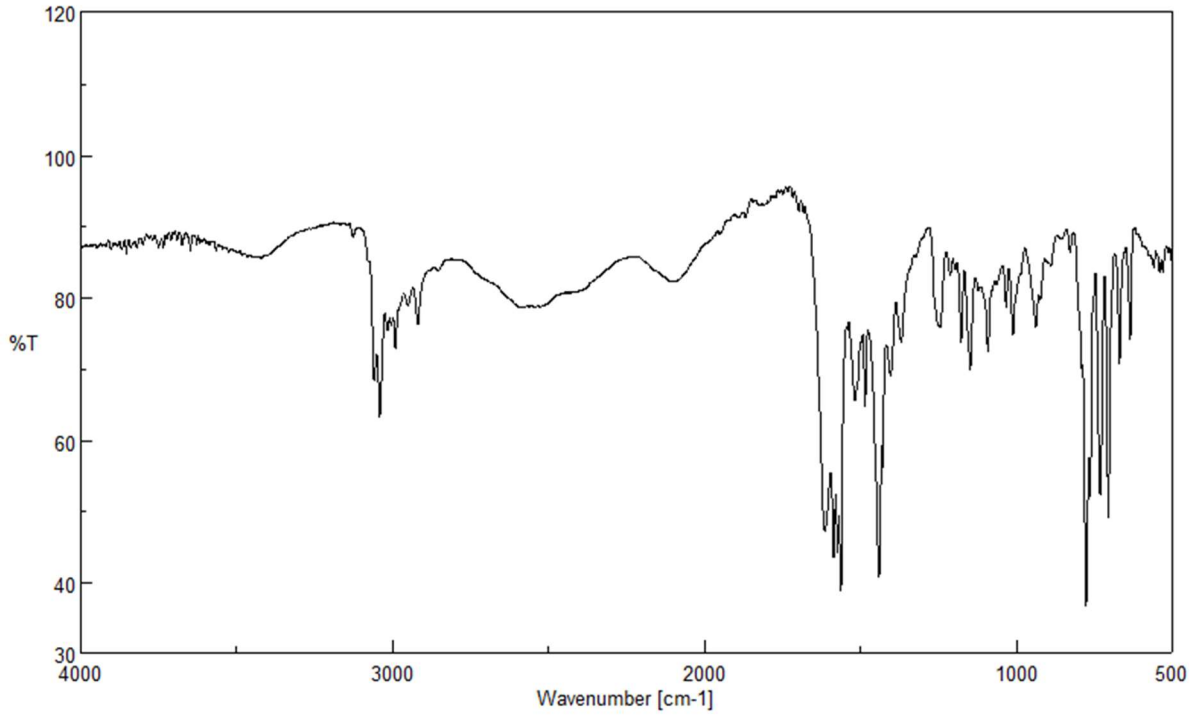

Fig. S4 FT/IR(KBr) spectrum of H[PhB(Py^{Me})$_3$] (H-**1**) at room temperature.

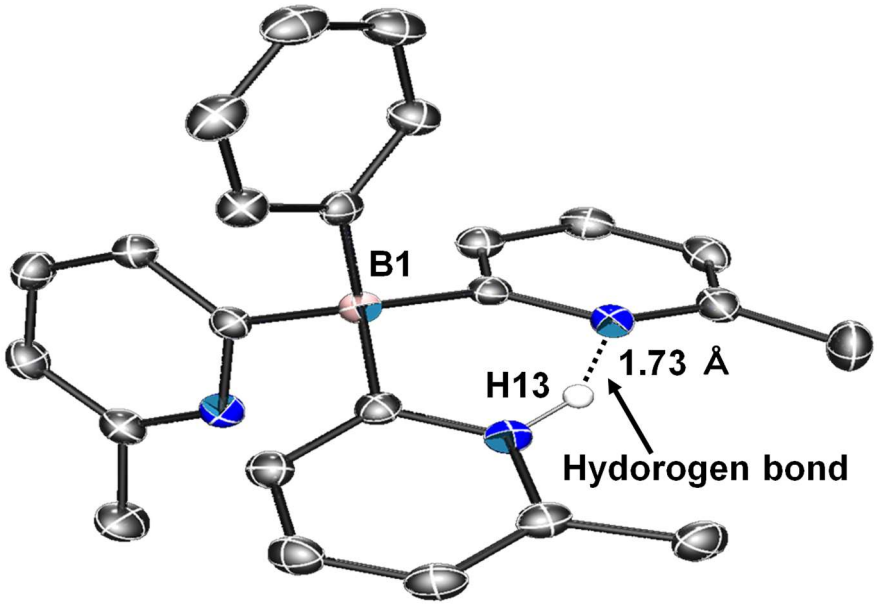

Fig. S5 Molecular structure of H[PhB(Py^{Me})$_3$] (H-**1**). Thermal ellipsoids are set at 30% probability. Hydrogen atoms except the nitrogen-attached one are omitted for clarity.

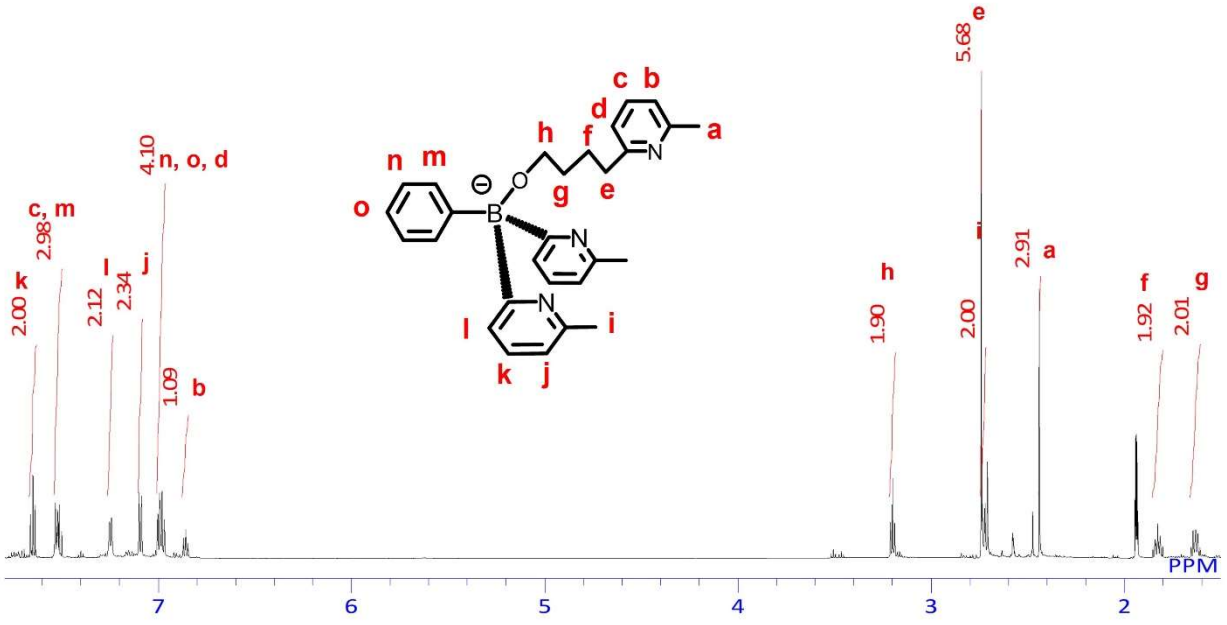

Fig. S6 ^{1}H NMR spectrum of H[PhB(OC_4H_8-Py^{Me})(Py^{Me})$_2$] (H-**2**) in CD_3CN at room temperature (600 MHz).

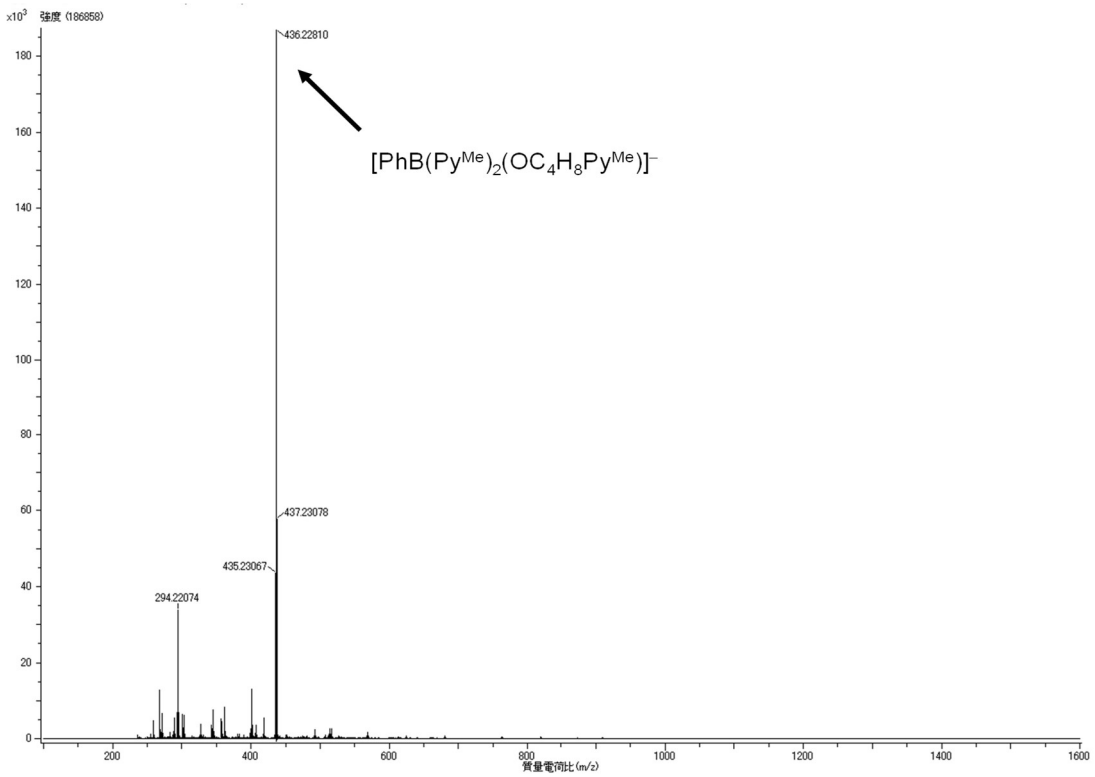

Fig. S7 ESI-MS(+) spectrum of H[PhB(OC_4H_8-Py^{Me})(Py^{Me})$_2$] (H-**2**) in MeOH.

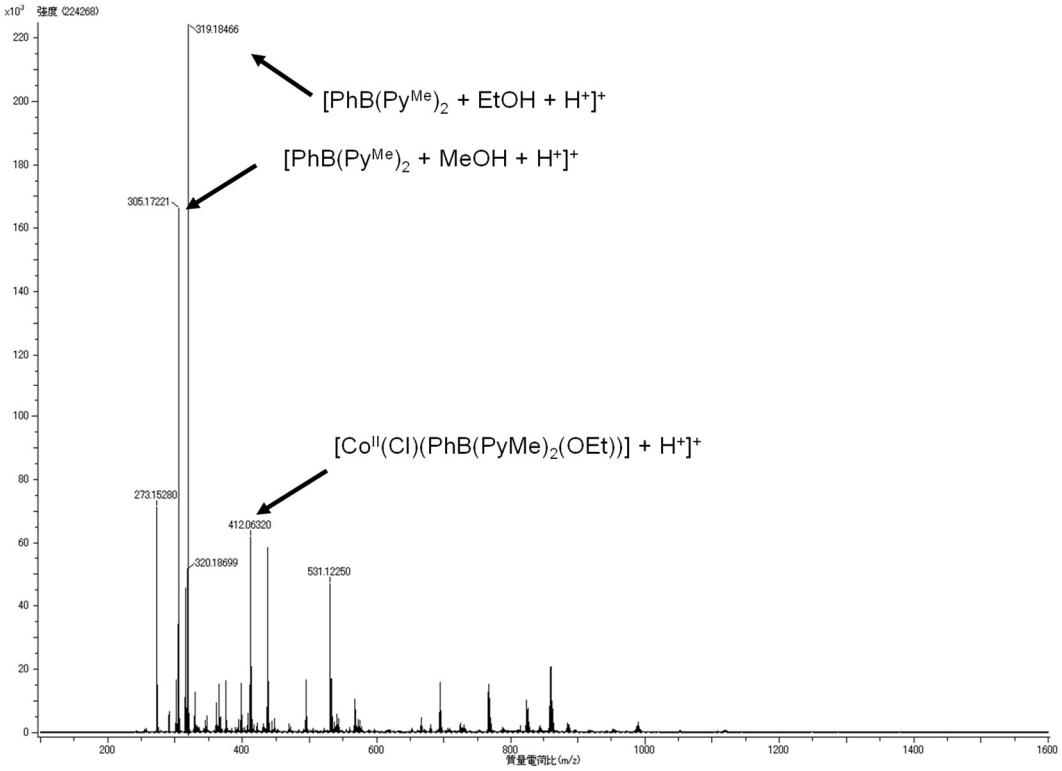

Fig. S8 ESI-MS(+) spectrum of $[Co[PhB(OEt)(Py^{Me})(Py^{Me}H)]Cl_2]$ (**3**) in MeOH.

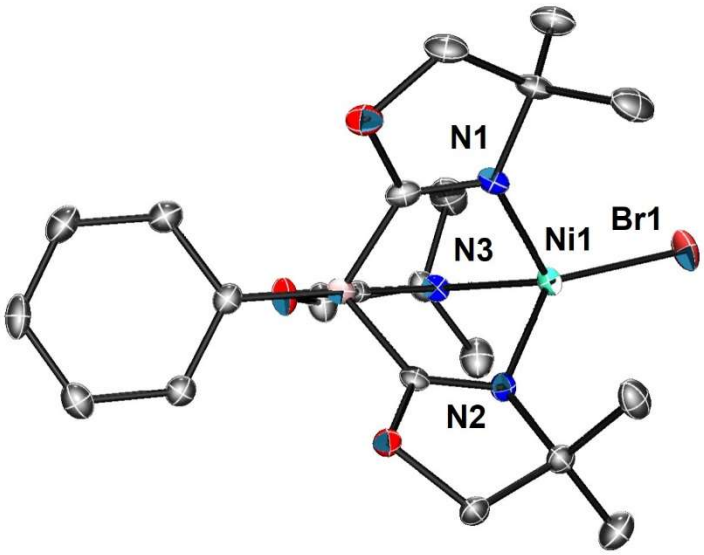

Fig. S9 Molecular structure of $[Ni^{II}Br(To^{M})]$ (**5**). Thermal ellipsoids are set at 30% probability. Hydrogen atoms are omitted for clarity.

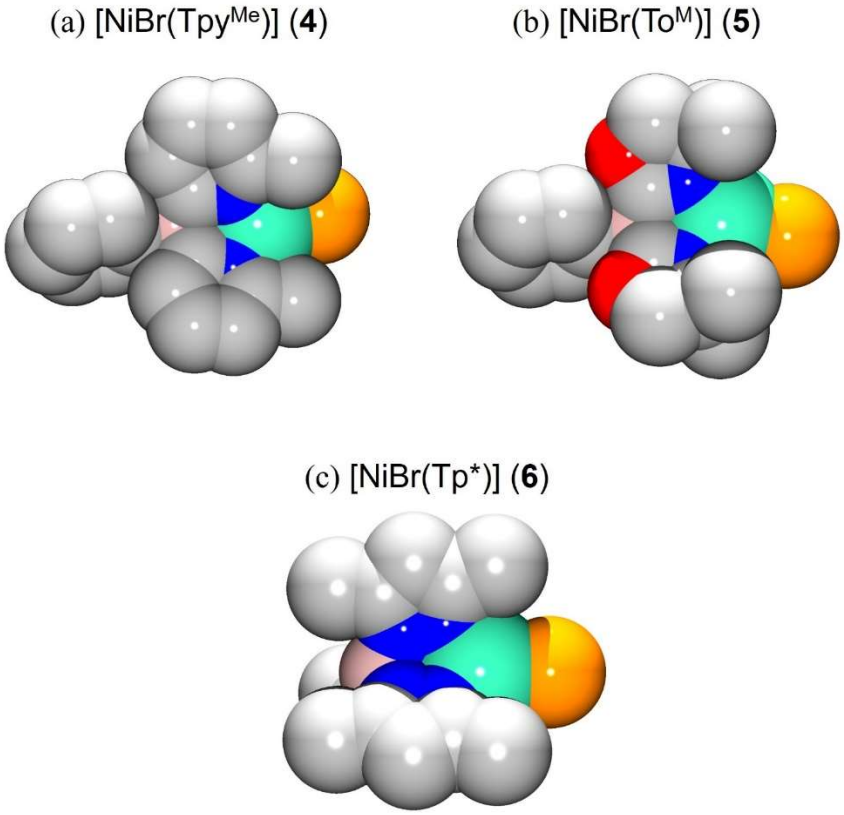

Fig. S10 Space-filling diagrams of **4**, **5**, and **6**. The colors of each elements are as follows. B: pink, Br; orange, C: gray, N: blue, Ni: emerald green, O: red.

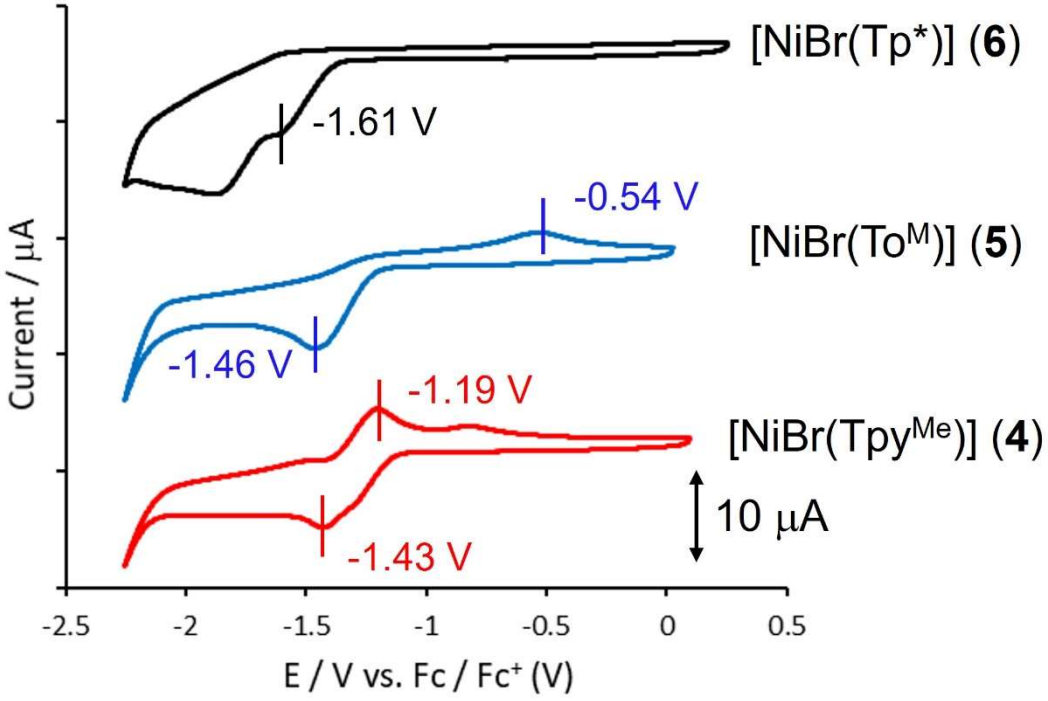

Fig. S11 Cyclic voltammograms of **4** – **6** in CH_2Cl_2 with 0.1 M $^n Bu_4NPF_6$.

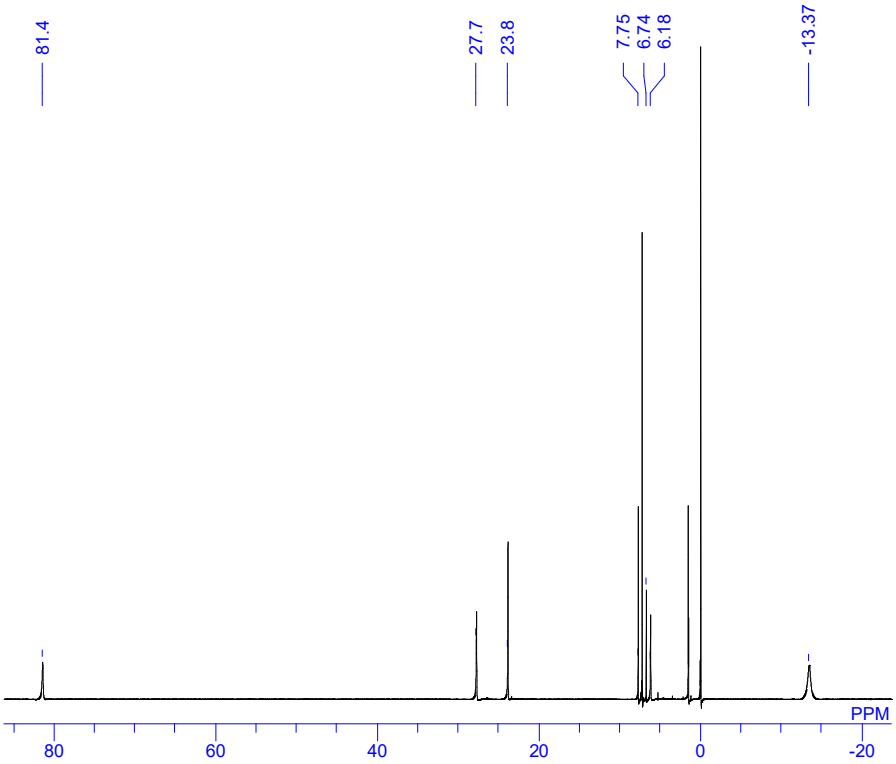

Fig. S12 ^{1}H NMR spectrum of [Ni^{II}Br(Tpy^{Me})] (**4**) in $CDCl_3$ at room temperature (600 MHz).

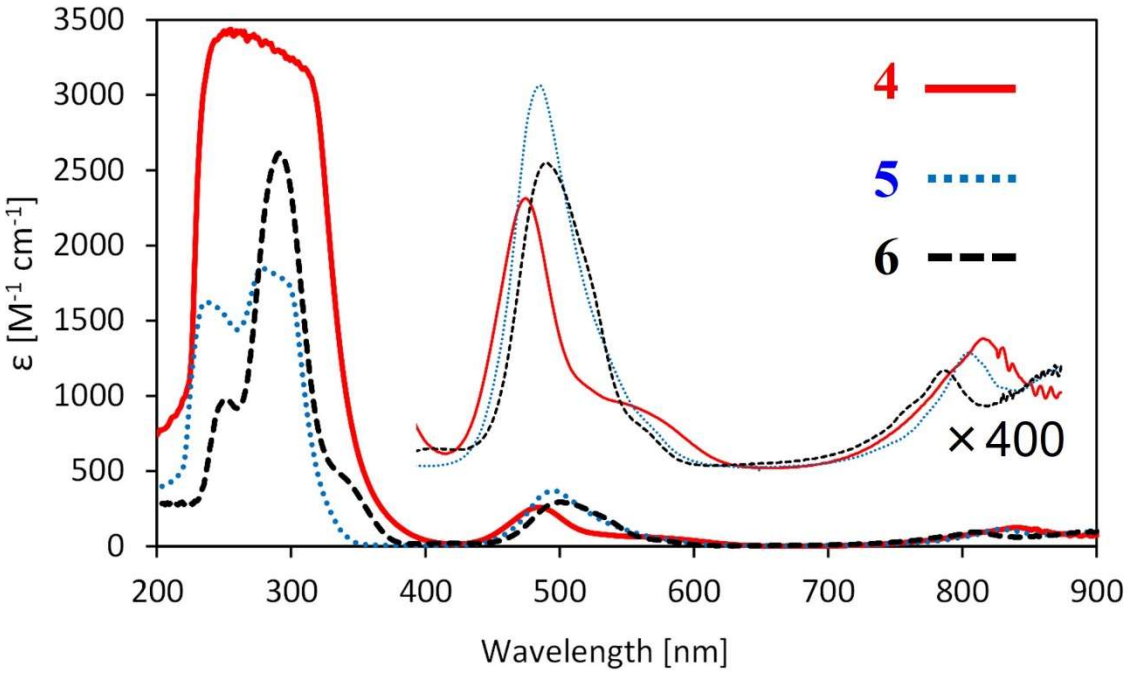

Fig. S13 UV-vis spectra of **4** – **6** in CH_2Cl_2 at room temperature.

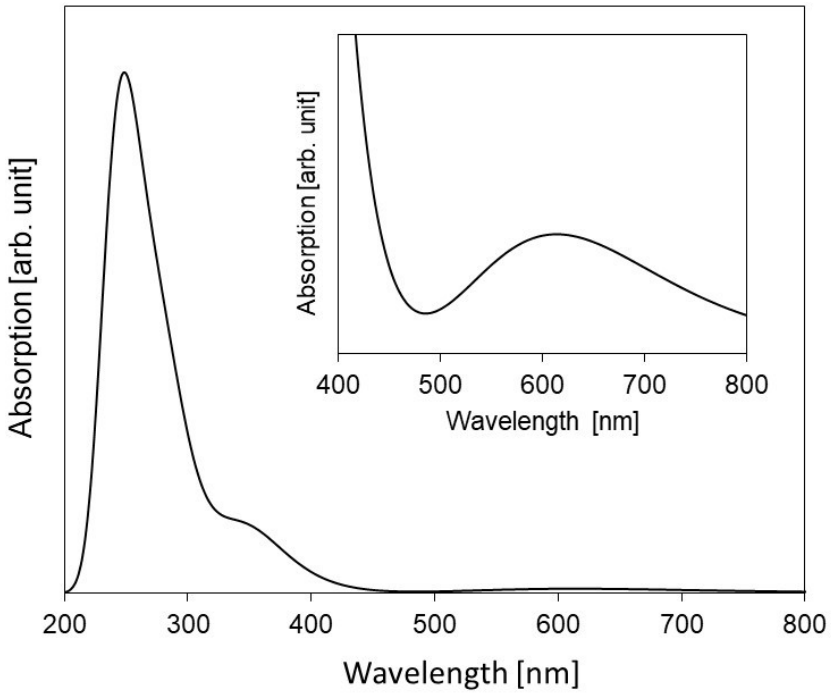

Fig. S14. Simulated absorption spectra of **4** calculated by the UB3LYP level of TD-DFT using def2TZVP for Ni and def2SVP for C, H, B, N, and Br.

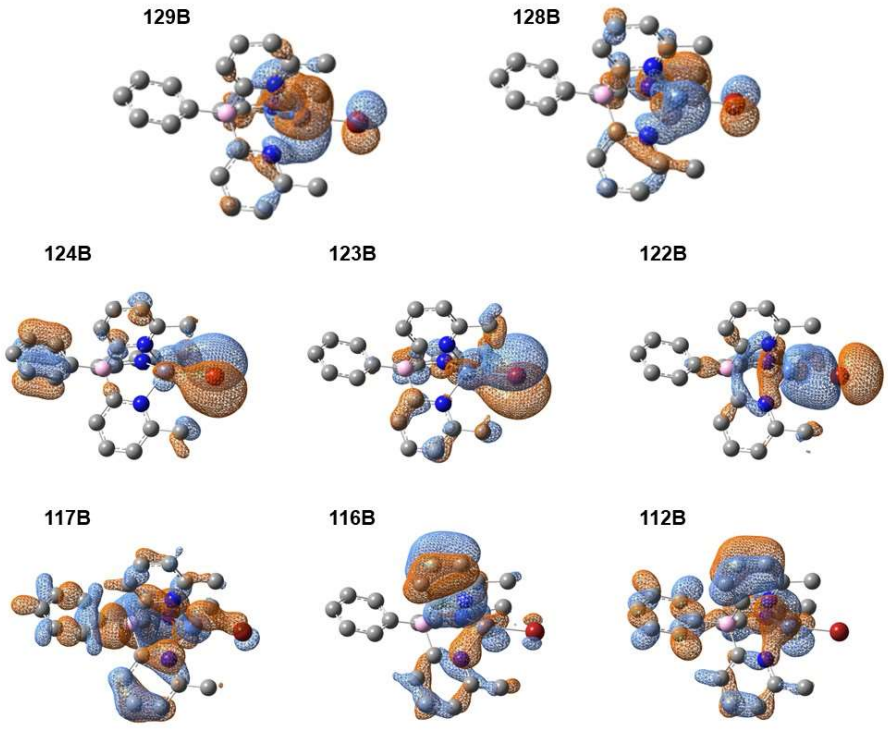

Fig S15. Selected molecular orbitals of **4** calculated by the UB3LYP level of TD-DFT using def2TZVP for Ni and def2SVP for C, H, B, N, and Br. The molecular orbitals of (117B, 116B, 112B) are distributed in the π orbitals of pyridine moieties as well as nickel d-orbital (bonded to the Br ligand).

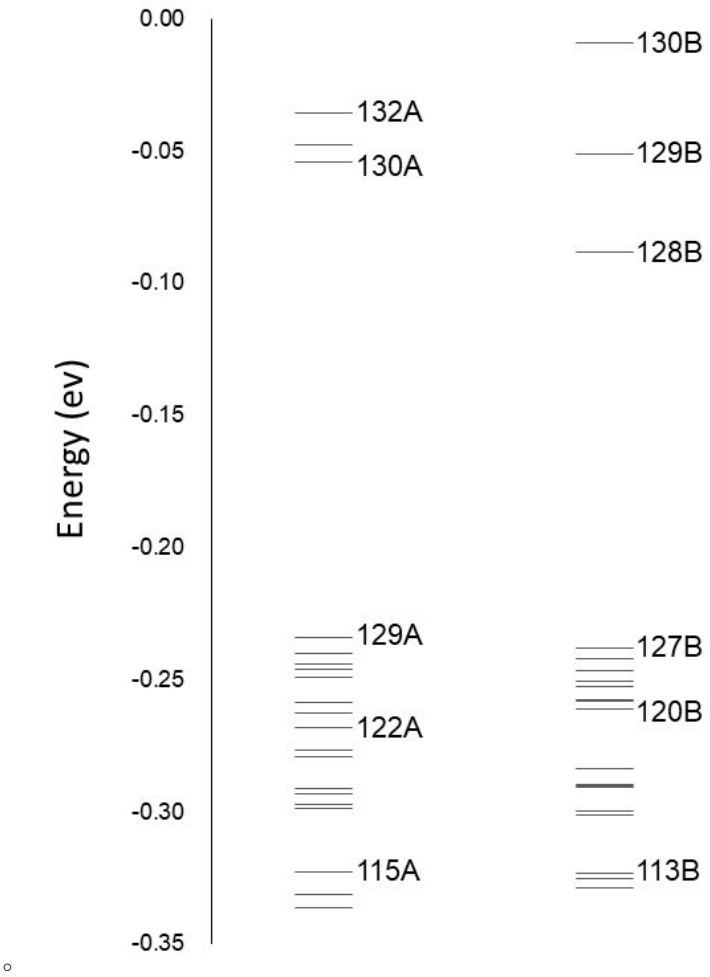

Fig. S16 Energy diagrams of molecular orbital of **4** calculated by the UB3LYP level of DFT using def2TZVP for Ni and def2SVP for C, H, B, N, and Br. Orbitals of 129B and 128B are the singly occupied molecular orbital (SOMO) of nickel (d_{xz} and d_{yz}).

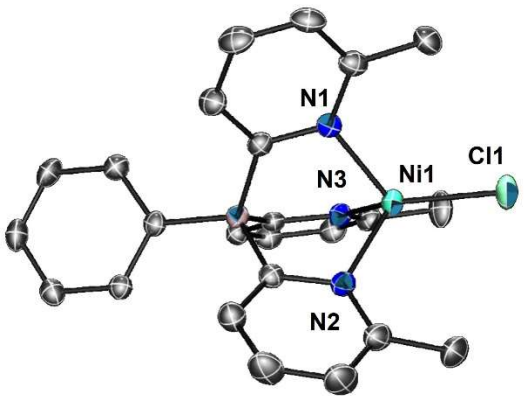

Fig. S17 Molecular structure of [$Ni^{II}Cl(Tpy^{Me}$)] (**7**). Thermal ellipsoids are set at 30% probability. Hydrogen atoms are omitted for clarity.

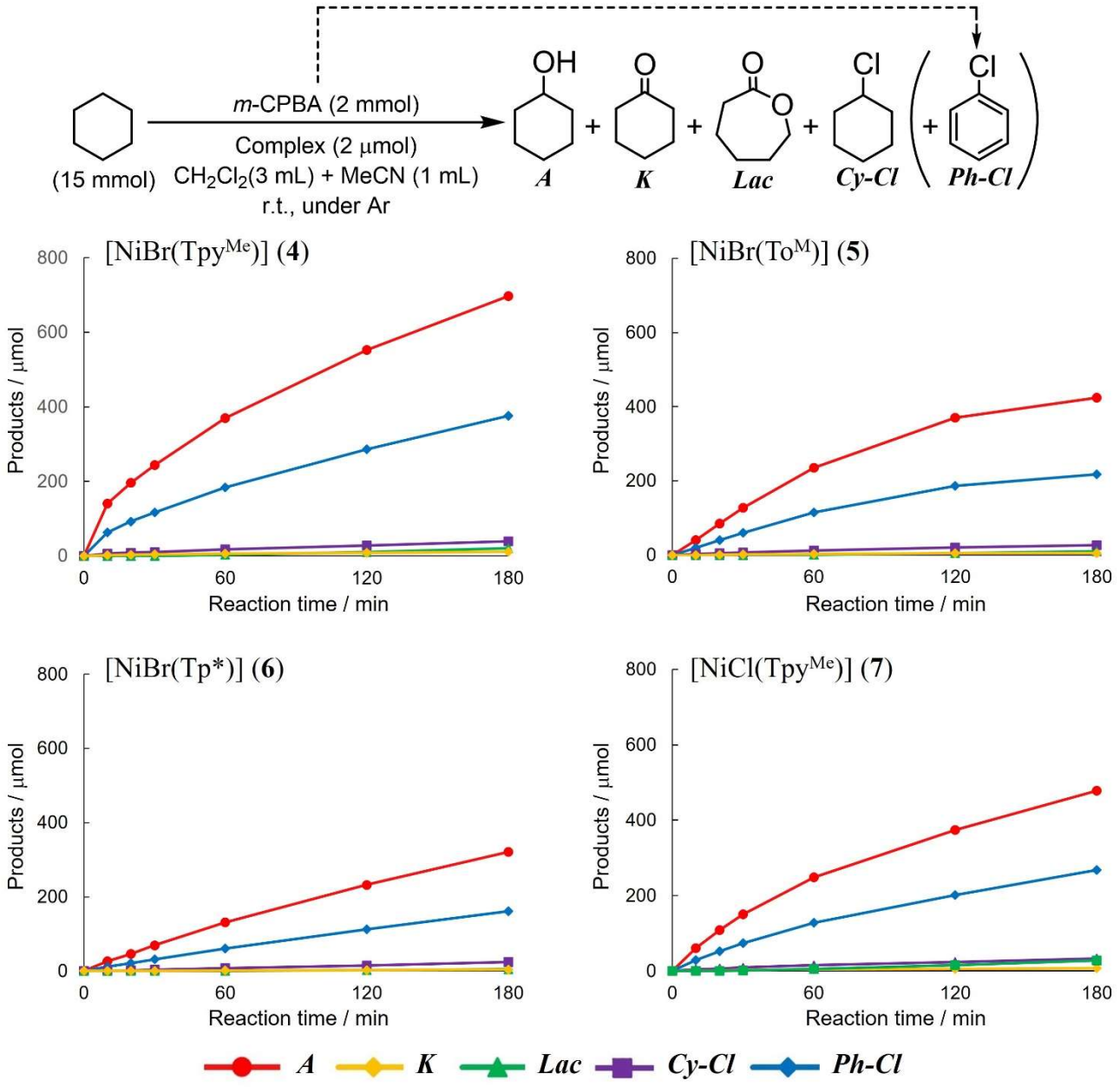

Fig. S18 Time course of cyclohexane oxidation with *m*CPBA catalyzed by the nickel(II) complexes **4** – **7**.

Table S1 Crystallographic data for **1**, **3**, **4**, **5** and **7**.

Compound	**1**	**3**	**4**
Formula	$C_{24}H_{24}BN_3$	$C_{20}H_{23}BCl_2CoN_2O$	$C_{25}H_{23}BBrN_3Ni$
Formula Weight	365.27	448.04	504.08
Space Group	$P2_1/n$	$P2_1/c$	$P2_1/n$
Crystal System	monoclinic	monoclinic	monoclinic
a / Å	13.1227(4)	7.3720(2)	9.9893(2)
b / Å	9.2714(3)	26.7621(6)	15.9480(3)
c / Å	16.9147(5)	11.1119(3)	13.6069(3)
α / °	90	90	90
β / °	101.238(3)	108.356(3)	91.906(2)
γ / Å	90	90	90
V / Å^3	2018.48(11)	2080.72(10)	2166.51(8)
Z	4	4	4
F(000)	776	924	1024
D(calced) / g·cm^{-1}	1.202	1.430	1.542
Temp. / K	293(2)	90	90
μ / cm^{-1}	0.542	8.917	3.562
θ_{max} / °	76.352 (CuKα)	76.516 (CuKα)	76.124 (CuKα)
Unique reflections	4095	4250	4406
Observed reflections ($I > 2\sigma(I)$)	3795	4157	4290
Parameters	260	247	280
R ($I > 2\sigma(I)$) / all [(a)]	0.0379 / 0.0401	0.0323 / 0.0331	0.0268 / 0.0274
wR ($I > 2\sigma(I)$) / all [(a)]	0.0960 / 0.0976	0.0795 / 0.0800	0.0679 / 0.0682
Goodness of fit S [(b)]	1.050	1.096	1.004

(a) $R = \Sigma||F_o| - |F_c|| / \Sigma|Fo|$. $R_w = \{\Sigma[w(Fo^2 - Fc^2)^2] / \Sigma[w(Fo^2)^2]\}^{1/2}$.

(b) $S = \{\Sigma[w(Fo^2 - Fc^2)^2] / (n - p)\}^{1/2}$, where n is the number of reflections and p is the total number of parameters refined.

Table S1 (continued).

Compound	**5**	**7**
Formula	$C_{21}H_{29}BBrN_3NiO_3$	$C_{25}H_{23}BClN_3Ni$
Formula Weight	520.90	458.42
Space Group	$P2_1/c$	$P2_1/n$
Crystal System	monoclinic	monoclinic
a / Å	11.0336(5)	10.03979(17)
b / Å	13.2310(4)	15.8652(2)
c / Å	16.0271(10)	13.3756(2)
α / °	90	90
β / °	95.895(3)	90.3207(15)
γ / Å	90	90
V / Å^3	2327.35(19)	2130.47(6)
Z	4	4
F(000)	1072	952
D(calced) / g·cm^{-1}	1.487	1.429
Temp. / K	113(2)	90
μ / cm^{-1}	2.577	2.578
θ_{max} / °	27.4831 (MoKα)	76.791 (CuKα)
Unique reflections	5213	4165
Observed reflections ($I > 2\sigma(I)$)	4137	3755
Parameters	271	274
R ($I > 2\sigma(I)$) / all [(a)]	0.0236 / 0.0307	0.0320 / 0.0353
wR ($I > 2\sigma(I)$) / all [(a)]	0.0511 / 0.0530	0.0829 / 0.0852
Goodness of fit S [(b)]	0.978	1.079

(a) $R = \Sigma||F_o| - |F_c|| / \Sigma|Fo|$. $R_w = \{\Sigma[w(Fo^2 - Fc^2)^2] / \Sigma[w(Fo^2)^2]\}^{1/2}$.

(b) $S = \{\Sigma[w(Fo^2 - Fc^2)^2] / (n - p)\}^{1/2}$, where n is the number of reflections and p is the total number of parameters refined.

Table S2. Selected bond length (Å) and angles (°) for **1**.

		Bond length (Å)			
B1–C1	1.6416(15)	B1–C8	1.6310(16)	B1–C14	1.6361(15)
B1–C20	1.6465(15)	N13–H13	0.986(17)		
		Bond angles (°)			
C1–B1–C8	111.41(9)	C1–B1–C14	109.00(8)	C1–B1–C20	109.53(8)
C8–B1–C14	108.62(9)	C8–B1–C20	106.89(9)	C14–B1–C20	111.39(8)

Table S3. Selected bond length (Å) and angles (°) for **2**.

		Bond length (Å)			
Co1–Cl1	2.2378(5)	Co1–Cl2	2.2617(5)	Co1–O1	1.9869(13)
Co1–N1	2.0183(16)				
		Bond angles (°)			
Cl1–Co1–Cl2	112.61(2)	Cl1–Co1–O1	120.22(4)	Cl1–Co1–N1	116.27(5)
Cl2–Co1–O1	101.93(4)	Cl2–Co1–N1	117.71(5)	O1–Co1–N1	84.77(6)

Table S4. Structural parameters for the nickel(II)-bromide complexes **4** – **6**. The planes (drawn in plane red) indicate the the least square planes defined by the carbon atoms of the nickel-surrounding methyl groups

[NiBr(Tpy^{Me})] (**4**) [NiBr(To^{M})] (**5**) [NiBr(Tp*)] (**6**)

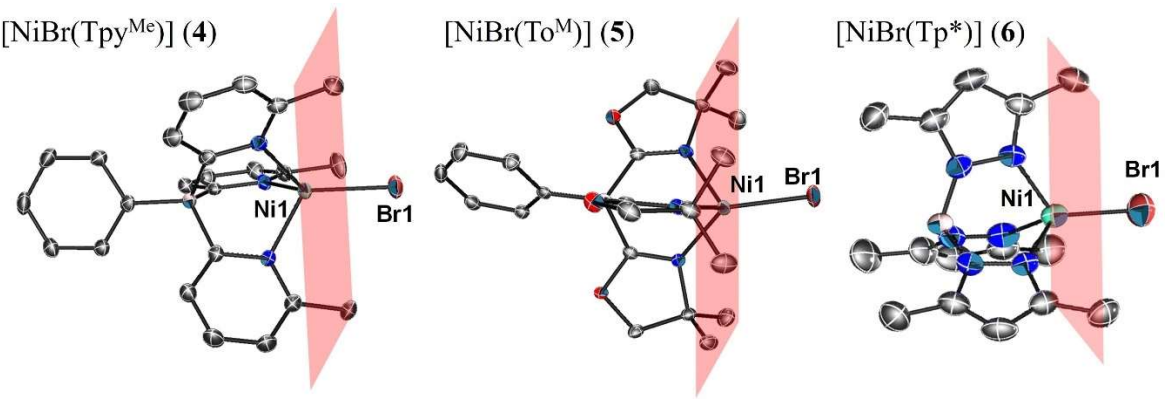

Complex (Borate ligand)	**4** (Tpy^{Me})	**5** (To^{M})	**6** (Tp*) [a] (molecule 1)	**6** (Tp*) [a] (molecule 2)
Bond lengths (Å)				
Ni – Br	2.3631(3)	2.3178(3)	2.2928(13)	2.2887(13)
Ni – N1	2.0285(14)	1.9983(13)	1.968(4)	1.966(4)
Ni – N2	2.0355(15)	1.9943(13)	1.968(4)	1.966(4)
Ni – N3	1.9666(15)	1.9823(13)	1.957(6)	1.987(5)
Avg. Ni – N	2.01	1.99	1.96	1.97
Bond angles (deg)				
Br – Ni –N1	118.18(4)	135.33(4)	124.00(12)	124.80(13)
Br – Ni – N2	117.56(4)	119.76(4)	124.00(12)	124.80(13)
Br –Ni – N3	130.18(4)	115.81(4)	122.77(19)	120.81(17)
N1 – Ni –N2	96.76(6)	90.15(5)	91.3(2)	91.3(2)
N1 – Ni – N3	94.58(6)	92.37(5)	92.88(17)	93.14(16)
N2 – Ni – N3	92.13(6)	93.43(5)	92.88(17)	93.14(16)
Avg. N – Ni – N	94.5	92.0	92.4	92.5
Distance betwen Br and the least square plane (Å)	1.419	2.215	1.769	1.774
Ni sphere shielded percentage by the borate ligand (%) [b]	65.36	63.74	60.18	59.91
Equivalent cone angle (deg) [b]	215.78	211.98	203.48	202.87

[a] from ref. 2

[b] determined by solid angle analysis (ref. 15)

Table S5. Selected bond length (Å) and angles (°) for the nickel(II)-chloride complexes [$Ni^{II}Cl(Tpy^{Me})$] (**7**), [$Ni^{II}Cl(To^{M})$] and [$Ni^{II}Cl(Tp^{*})$].

Complex (Borate ligand)	[$Ni^{II}Cl(Tpy^{Me})$] (**7**)	[$Ni^{II}Cl(To^{M})$] [a]	[$Ni^{II}Cl(Tp^{*})$] [b] (molecule 1)	[$Ni^{II}Cl(Tp^{*})$] [b] (molecule 2)
Bond lengths (Å)				
Ni – Cl	2.2204(5)	2.1851(5)	2.1955(18)	2.150(2)
Ni – N1	2.0229(13)	2.0002(11)	1.964(3)	1.992(3)
Ni – N2	1.9623(13)	1.9982(11)	1.964(3)	1.992(3)
Ni – N3	2.9269(14)	1.9825(11)	1.962(5)	1.992(5)
Bond angles (deg)				
Cl – Ni –N1	117.47(4)	136.75(3)	123.66(10)	125.44(11)
Cl – Ni – N2	132.52(4)	119.62(4)	123.66(10)	125.44(11)
Cl –Ni – N3	116.37(4)	114.91(3)	122.39(16)	121.63(15)
N1 – Ni –N2	93.68(5)	89.79(5)	91.47(18)	90.30(19)
N1 – Ni – N3	96.78(5)	92.22(4)	93.51(14)	92.16(14)
N2 – Ni – N3	92.26(6)	93.12(5)	93.51(14)	92.16(14)

[a] from ref. 16

[b] from ref. 17

Table S6. Selected electronic transitions of **4** in the visible region calculated by the UB3LYP level of TD-DFT using def2TZVP for Ni and def2SVP for C, H, B, N, and Br.

λ[nm]	Oscillator strength *f*	Transition with Maximum CI coefficient	|CI coefficient|
665.89	0.0020	112B → 128B	0.44043
		116B → 128B	0.37493
		122B → 128B	0.45763
		124B → 128B	0.30942
595.17	0.0055	113B → 129B	0.59665
		117B → 129B	0.46066
		118B → 129B	0.31916
		123B → 129B	0.34109
390.53	0.0028	126B → 128B	0.93001
383.50	0.0079	123B → 128B	0.38527
		124B → 128B	0.69892
		125B → 128B	0.33025
344.99	0.0815	123B → 129B	0.76400
		124B → 129B	0.39729

Table S7. Cyclohexane oxidation with *m*CPBA mediated by the nickel(II) complexes **4** – **7**.

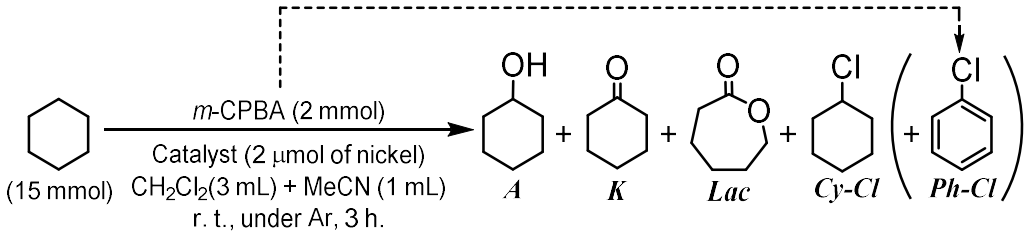

Complex	Products / μmol					TON[1]	***A*/(*K*+ *Lac*)**
	A	***K***	***Lac***	***Cy-Cl***	***Ph-Cl***		
4	697.6	11.7	20.5	39.6	375.8	401	22
5	424.3	5.2	9.8	26.8	217.8	241	28
6	320.6	3.4	4.5	23.9	160.8	180	40
7	478.0	7.4	27.8	32.9	268.0	291	14

[1] TON = (***A*** + 2 × ***K*** + 2 × ***Lac*** + ***Cy-Cl***) / nickel

References

1. J. F. Dunne, J. Su, A. Ellern and A. D. Sadow, *Organometallics*, 2008, **27**, 2399–2401.
2. P. J. Desrochers, J. Telser, S. A. Zvyagin, A. Ozarowski, J. Krzystek and D. A. Vicic, *Inorg. Chem.*, 2006, **45**, 8930-8941.
3. O. V. Dolomanov, L. J. Bourhis, R. J. Gildea, J. A. K. Howard and H. Puschmann, *J. Appl. Cryst.*, 2009, **42**, 339–341.
4. Rigaku Corporation, Tokyo, Japan, 2008.
5. G. M. Sheldrick, *Acta Cryst.*, 2015, **A71**, 3–8.
6. G. M. Sheldrick, *Acta Cryst.*, 2015, **C71**, 3–8.
7. A. Altomare, G. Cascarano, C. Giacovazzo, A. Guagliardi, M. C. Burla, G. Polidori and M. Camalli, *J. Appl. Cryst.*, 1994, **27**, 435.
8. G. M. Sheldrick, *Acta Cryst.*, 2008, **A64**, 112–122.
9. L. J. Farrugia, *J. Appl. Cryst.*, 1999, **32**, 837–838.
10. Gaussian 16, **Revision C.01**, M. J. Frisch, G. W. Trucks, H. B. Schlegel, G. E. Scuseria, M. A. Robb, J. R. Cheeseman, G. Scalmani, V. Barone, G. A. Petersson, H. Nakatsuji, X. Li, M. Caricato, A. V. Marenich, J. Bloino, B. G. Janesko, R. Gomperts, B. Mennucci, H. P. Hratchian, J. V. Ortiz, A. F. Izmaylov, J. L. Sonnenberg, D. Williams-Young, F. Ding, F. Lipparini, F. Egidi, J. Goings, B. Peng, A. Petrone, T. Henderson, D. Ranasinghe, V. G. Zakrzewski, J. Gao, N. Rega, G. Zheng, W. Liang, M. Hada, M. Ehara, K. Toyota, R. Fukuda, J. Hasegawa, M. Ishida, T. Nakajima, Y. Honda, O. Kitao, H. Nakai, T. Vreven, K. Throssell, J. A. Montgomery, Jr., J. E. Peralta, F. Ogliaro, M. J. Bearpark, J. J. Heyd, E. N. Brothers, K. N. Kudin, V. N. Staroverov, T. A. Keith, R. Kobayashi, J. Normand, K. Raghavachari, A. P. Rendell, J. C. Burant, S. S. Iyengar, J. Tomasi, M. Cossi, J. M. Millam, M. Klene, C. Adamo, R. Cammi, J. W. Ochterski, R. L. Martin, K. Morokuma, O. Farkas, J. B. Foresman, and D. J. Fox, *Gaussian, Inc.*, Wallingford CT, **2016**.
11. F. Weigend and R. Ahlrichs, *Phys. Chem. Chem. Phys.*, 2005, **7**, 3297–305.
12. GaussView, **Version 6.1**, Roy Dennington, Todd A. Keith, and John M. Millam, *Semichem Inc.*, Shawnee Mission, KS, **2016**.
13. Cossi, M.; Scalmani, G.; Rega, N.; Barone, V. *J. Chem. Phys.*, 2002, **117**, 43.
14. M. E. Casida, C. Jamorski, K. C. Casida, D. R. Salahub, *J. Chem. Phys.*, 1998, **108**, 4439. (b) R. E. Statmann, G. E. J. Scuseria, *Chem. Phys.*, 1998, **109**, 8218. (c) R. Bauernschmitt, R. Ahlrichs, *Chem. Phys. Lett.*, 1996, **256**, 454–464.
15. I. A. Guzei and M. Wendt, *Dalton Trans.*, 2006, 3991–3999.
16. T. Takayama, J. NakaZawa and S. Hikichi, *Acta Cryst.*, 2016, **C72**, 842–845.
17. P. J. Desrochers, S. LeLievre, R. J. Johnson, B. T. Lamb, A. L. Phelps, A. W. Cordes, W. Gu, and S. P. Cramer, *Inorg. Chem.*, 2003, **42**, 7945–7950.